BeBeC-2014-11

SODIX IN COMPARISON WITH VARIOUS DECONVOLUTION METHODS

Stefan Funke[1], Robert P. Dougherty[2] and Ulf Michel[3]
[1]DLR Institute of Propulsion Technology, Engine Acoustics Department
Müller-Breslau-Str. 8, 10623 Berlin, Germany
[2]OptiNav Inc., Bellevue, WA, USA
[3]CFD Software E+F GmbH, Berlin, Germany

Abstract

SODIX is a method for the localization of sound sources including the quantification of their directivities. Other source localization methods commonly assume point monopole sources with uniform directivity. The performance of SODIX is compared in this paper with previously published results [9] of conventional delay-and-sum beamforming and the advanced deconvolution methods DAMAS, DAMAS2, CLEAN-SC, TIDY, and LPD by using the same set of array data. The results show that the resolution of SODIX is only slightly inferior to those of the best advanced beamforming methods.

1 INTRODUCTION

SODIX is a source localization method that is capable of determining the directivities of all sources in a source distribution [11–13] from the signals of a large microphone array. The angular range for the directivities is defined by the locations of the array microphones with respect to the sources. Other localization methods commonly assume that the sources are monopoles. SODIX's advantage is useful, whenever sources exhibit strong directivities as is the case with aircraft engines.

SODIX (*SOurce Directivity modeling in cross-spectral-matriX*) is based on the cross-spectral density matrix (CSM) of the signals of an array of microphones The method does not use a beamform map as an intermediate step as required by deconvolution methods. The method was developed for situations with sources that have a strong directivity, like a turbofan engine. Open air noise tests of these engines are very expensive which justifies the installation of microphone arrays consisting of a large number of microphones. A test setup is shown in Fig. 1. An engine is mounted above the ground plane. Far-field microphones are installed on a circle around the engine in a distance of 45.72 m in steps of 5 deg. These are used to measure the directivity of

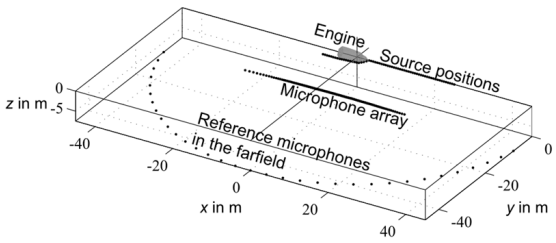

Figure 1: Schematic of the measurement setup showing the linear grid with point sources along the engine, the linear microphone array, and the far-field microphones at a distance of 45.72 m. The engine is mounted 5 m above the ground.[11]

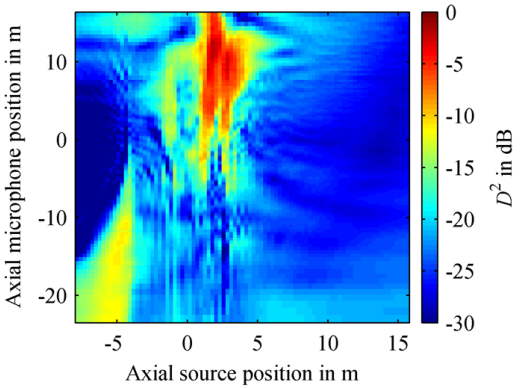

Figure 2: Source strengths for the 500 Hz one-third octave band computed with SODIX. The directivity of each source position (shown on the horizontal axis) is shown on the vertical axis as function of the microphone position. The color coded dynamic range in this plot is 30 dB. [11]

the sound but the contributions of the various sources on the engine cannot be determined. This is the task of SODIX, which uses a line array of microphones with a length of roughly 43 m in the shown example, mounted on the ground approximately parallel to the engine axis.

A characteristic result of SODIX is shown in Fig. 2. The directivity of each source position on the horizontal axis is plotted on the vertical axis as function of the microphone position. The results are shown for the 500 Hz one-third octave band and the color coded dynamic range in this plot is 30 dB [11]. The primary and secondary nozzles can be identified around the real positions x=1.2 m and x=2.2 m, they are the loudest noise sources of the engine because it is run at low power in this case. Nevertheless, jet noise can be identified for $x > 2.5$ m peaking at microphone positions around $x = 9$ m and $x = 12$ m and even the "cone of silence" is visible for $x > 13$ m on the vertical axis. The engine inlet is located at $x = -4.3$ m. A further source on the engine nacelle is visible at $x = -1$ m. Detailed discussions can be found in [11–13].

It has not yet been studied how the capability to determine directivities affects the localization quality of SODIX in comparison to advanced beamforming methods, which are based on a deconvolution of beamforming maps. The performances of various such methods was compared by Dougherty, Ramachandran, and Raman (2013) [9]. The studied methods were conventional beamforming (CBF), DAMAS, DAMAS2, CLEAN-SC, TIDY and a new method called Linear Programming Deconvolution (LPD), which is based on a new deconvolution strategy. (All methods are described in section 2). An experimental test case was designed for this comparison. More details are given in section 3.

2 SODIX IN COMPARISON TO CLASSICAL BEAMFORMING AND ADVANCED INVERSE METHODS

Acoustic antennas with microphone arrays are commonly used whenever the locations and strengths of sound sources have to be determined. The microphone signals can be evaluated in various ways. In many situations the classical beamforming (CBF) method using the delay-and-sum algorithm is used. Classical beamforming can be carried out in the time domain or in the frequency domain. The time-domain method requires interpolation of the microphone signals to adjust for the time delays with respect to a focal point in the source region. In the frequency domain the complex power spectra of the microphone signals are added up by including a phase shift for each focal point. Both methods can be performed almost in real time with appropriate hardware. More common in the frequency domain are analysis methods based on the cross-spectral matrix (CSM) of the microphone signals, averaged over a longer time series.

Results of the classical beamforming are beamform maps which are the outcome of a convolution of the source distribution with the beam patterns of the sources with respect to the microphone positions. The beam pattern of a single monopole point source (also called point-spread function, PSF) depends strongly on the wave length of the sound, but also on the microphone positions, the weighting factors of the microphone signals, and on the source position. The interpretation of the resulting maps with respect to the locations and strengths of the sources can be very challenging. The width b of the main lobe of the point spread function is directly proportional to the wave length λ and to the distance L of the source from the array center and inversely proportional to the array diameter D as *seen* from the source. The strong dependence on λ has the consequence that broadband beamform maps can easily be dominated by the contributions of low-frequency sources. It is therefore advisable to perform the beamforming analysis as a function of frequency, e.g., in one-third octave bands or $1/12^{\text{th}}$ octave bands. But even then the interpretation of the beamform maps may be difficult especially if the sources are separated less than the Sparrow limit r_s. At the Sparrow limit two point sources of equal strength are no longer characterized in the map by two peaks, but can still be identified visually. The Sparrow limit is defined by [9]

$$r_s = 0.47\frac{\lambda}{\sin\theta}\,, \tag{1}$$

where θ is the half angle under which the phased array is seen from the source point. With $\sin\theta \approx D/(2L)$ we obtain for an array with diameter D

$$r_s \approx 0.94\frac{\lambda L}{D}\,. \tag{2}$$

For microphone arrays the actual factor (0.94) depends on the positions and the weighting factors of the microphones as well as on the positions of the sources.

The problems caused by the sidelobes of the beam patterns can be reduced or may even be completely avoided with inverse methods. Deconvolution methods ideally reverse the convolution that led to the beamform maps. A large number of source positions is assumed and the source strengths (based on monopole directivities) in each of these positions are determined such that the original beamform map is reproduced as well as possible by the sum of the beam-

form maps of all individual sources, which are assumed to be uncorrelated.

The first solution of this inverse problem was published by Brühl & Röder (2000) [6] under the name *source-density modeling* (SDM). The mathematical procedure for solving the problem iteratively is partly published in a technical report (1997)[5].

Brooks & Humphreys [3, 4] proposed in 2004 a fully documented procedure, which they called *deconvolution approach for the mapping of acoustic sources* (DAMAS). They solved the inverse problem with a modified Gauss-Seidel method by setting negative source strengths to zero after each iteration step. This way of considering the constraint of positive source strengths may be causal for the slow convergence of the method. For SDM as well as for DAMAS the beam patterns (PSF) have to be calculated for all source positions which consumes much time. This problem is addressed by DAMAS2 proposed by Dougherty [7], who uses a shift-invariant beam pattern (PSF) for all source positions, which is considered a good approximation for the real beam patterns. The associated error is accepted in return for a much shorter computing time. The invariance of the PSF permits use of FFT convolution to speed up the computation. Various iterative deconvolution methods are compared by Ehrenfried & Koop [10]. Included are solutions of DAMAS and DAMAS2 with a a gradient-type non-negative least-squares (NNLS) approach. In addition, embedded methods are proposed that allow a small variation of the PSF.

A new method called *linear programming deconvolution* (LPD) was developed by Dougherty 2013 and reported in [9]. The strategy of the previously described methods was to approximate the measured beamform maps with the maps of the modeled sources as well as possible using a least squares procedure. A substantial part of the values in the modeled beamform map will be larger than in the measured map. This is now changed to finding a solution with the constraint that the modeled beamform map nowhere exceeds the measured map. The reasoning behind this strategy is that each uncorrelated source yields a non-negative contribution to the beamform map and no source can cause the map to decrease in any point. This task can be efficiently solved by linear programming with the simplex algorithm.

One problem of the previously described deconvolution methods is that the PSF is estimated analytically and may deviate from the actual PSF for various reasons. Sijtsma 2007 [17–19] found a method to extract the actual PSF from the beamform maps from the cross-spectral matrix (CSM) of the microphone signals. The method is called CLEAN-SC (*CLEAN based on spatial source coherence*). It is assumed that the maximum in the beamform map is co-located with an actual source. (This assumption may not always be true.) The experimental PSF of this source is determined from the coherent part of the CSM in the neighboring source positions. This experimental beampattern is then subtracted from the original beamform map yielding a new cleaned beamform map, which is the basis of the next iterative step. A big advantage of CLEAN-SC is that its computational cost is much lower than for DAMAS. The uncertainty of the assumption that the peak value in the map is co-located with a source position may be reduced by applying orthogonal beamforming [16] before CLEAN-SC.

Dougherty developed a similar method called TIDY, which is based on the cross-correlation matrix (CCM) in the time domain rather than the CSM in the frequency domain. The method was first described 2009 by Dougherty & Podboy [8].

So far, only inverse methods based on the beamform maps were discussed. However, a different strategy of finding the locations and strengths of sources can be followed: modeling the cross-spectral density matrix (CSM) rather than the beamform map. This was proposed by Blacodon & Élias [1, 2] and called *spectral estimation method* (SEM). Cross-spectral matrices

are generated from point sources in each source grid point assuming uniform directivities of the sources. The amplitudes of the sources are then determined with a least-squares fit between the modeled and the measured cross-spectral matrices by minimizing the cost function F

$$F = \sum_{m,n=1}^{M} \left| C_{mn} - C_{mn}^{\mathrm{mod}} \right|^2 . \tag{3}$$

M is the number of microphones, C_{mn} is the measured CSM and C_{mn}^{mod} is the modeled CSM. The modeled CSM is defined by

$$C_{mn}^{\mathrm{mod}} = \sum_{j=1}^{J} g_{jm} A_j^2 g_{jn}^* \tag{4}$$

where A_j^2 is the strength of source j. g_{jm} are the steering vectors for each source $j = 1 \ldots J$ relative to the microphone m.

$$g_{jm} = \frac{1}{r_{jm}} e^{ikr_{jm}} \tag{5}$$

The g_{jm} not only describe the phase delays due to the propagation from the sources to the microphones, but also the amplitude decays due to spherical wave propagation. The solution of A_j is iteratively found by finding a minimum of the cost function F. Since the source strength is A_j^2 the solution is physically valid for any real value of A_j.

SODIX is an extension of SEM by allowing the sources to have a directivity [11–13]. The array consists of M microphones and a number of J source positions is assumed. It is assumed that every source in the $j = 1 \ldots J$ positions has an unknown directivity D_{jm} to each of the $m = 1 \ldots M$ microphone positions. The modeled CSM is then defined by

$$C_{mn}^{\mathrm{mod}} = \sum_{j=1}^{J} g_{jm} D_{jm} D_{jn} g_{jn}^* \tag{6}$$

with the directivity values $D_{jm} \geq 0$ and the steering vectors g_{jm} as defined in Eq. (5).

Since the number $J \times M$ of unknown real directivity values D_{jm} is generally larger than the number of M^2 independent real elements of the CSM, the problem of minimizing F according to Eq. (3) may often be ill-posed. Additional conditions are required to solve this problem. Therefore, it is assumed that the directivities D_{jm} for each source j are relatively smooth for neighboring microphones m and that the D_{jm} for a given microphone number m are smooth for neighboring source positions j. To account for this, the cost function is appended by two smoothing functions $G_{\mathrm{d}}(D_{jm})$ and $G_{\mathrm{s}}(D_{jm})$, where G_{d} describes the smoothing of the directivities for each source position j and G_{s} describes the smoothing of the source strengths seen by the microphone m for neighboring source positions.

$$F = \sum_{m,n=1}^{M} \left| C_{mn} - C_{mn}^{\mathrm{mod}} \right|^2 + \sigma_{\mathrm{d}} G_{\mathrm{d}} + \sigma_{\mathrm{s}} G_{\mathrm{s}} \tag{7}$$

The intensity of the smoothing can be controlled with the slack variables σ_{d} and σ_{s}. A large value for σ_{d} would force the directivities to become more uniform, a large value for σ_{s} would

make the source distribution more uniform.

SODIX was originally developed for a line array [12, 13] and later extended to 2D or 3D source distributions and 2D or 3D arrays [11]. In addition, the definition of the modeled CSM was changed to

$$C_{mn}^{\mathrm{mod}} = \sum_{j=1}^{J} g_{jm}\, d_{jm}^2\, d_{jn}^2\, g_{jn}^* \,. \tag{8}$$

The constraint of positive source strengths $D_{jm} = d_{jm}^2$ is automatically satisfied for any real valued d_{jm}, which simplifies minimizing F in Eq. (7).

To allow for multi-dimensional source grids and microphone arrangements new definitions of the smoothing functions were introduced in [11].

$$G_{\mathrm{d}}(d) = \sum_{j=1}^{J} \sum_{m=1}^{M} \sum_{l=1}^{L(m)} \alpha_l \left(d_{jm}^2 - d_{j,\Lambda(l)}^2 \right)^2 \quad \text{and} \tag{9}$$

$$G_{\mathrm{s}}(d) = \sum_{m=1}^{M} \sum_{j=1}^{J} \sum_{k=1}^{K(j)} \alpha_k \left(d_{jm}^2 - d_{\kappa(k),m}^2 \right)^2 . \tag{10}$$

L is here the number of nearby microphones in the array and K is the number of nearby sources in the source region within a sphere with radius r_{mic}, respectively r_{src}. The variables Λ and κ hold the indices of the microphones and the sources that are located inside the particular sphere around a microphone l and a source k. Finally, α is a linear weighting with respect to the distance of a microphone or a source inside a sphere to the microphone or the source in the center of a sphere.

$$\alpha_l = 1 - \frac{r(l)}{r_{\mathrm{mic}}} \tag{11}$$

$$\alpha_k = 1 - \frac{r(k)}{r_{\mathrm{src}}} \tag{12}$$

Minimizing the cost function (7) is achieved by evaluating the partial derivatives of F with respect to the directivity values d_{jm}.

$$\frac{\partial F}{\partial d_{jm}} = 0 \tag{13}$$

This results in a set of JM non-linear equations for the unknowns d_{jm}. The conjugate gradient method of Rasmussen[15] is used to solve this nonlinear problem. The iterative solution is very robust and may be started for each microphone m and each frequency band with a uniform source distribution $d_{jm} = \text{const.}$, which reproduces the measured sound pressure level.

It is shown in reference [11] that the solution converges rather fast and is practically independent on the initial source distribution. The smoothing functions seem to suppress spurious sources. It is surprising that the solution converges even without the use of the smoothing functions ($\sigma_{\mathrm{d}} = \sigma_{\mathrm{s}} = 0$). A removal of the main-diagonal of the cross-spectral matrix results in a reduced dynamic range of the source levels, but the absolute levels of the dominant sources are preserved. This should make SODIX suitable for measurements in wind tunnels where turbulence induces spurious noise on the microphones, yielding high levels of the main diagonal of

Figure 3: Test setup with an OptiNav 24 Jr microphone array[9].

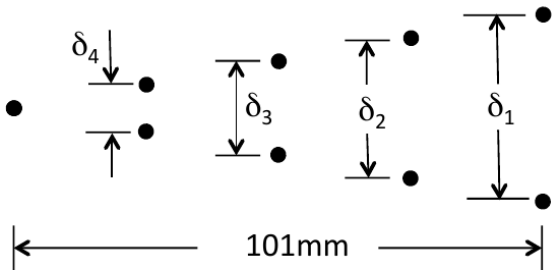

Figure 4: V-shaped pattern of holes for noise sources [9].

the cross-spectral density matrix CSM.

3 RESULTS FROM EXPERIMENTAL DATA

The experimental data set that will be used here was generated and first used by Dougherty, Ramachandran, and Raman [9]. They investigated the resolution of a new linear programming deconvolution (LPD) approach and compared it with results from conventional beamforming and various other deconvolution methods.

3.1 Data set

The experimental setup is shown in Fig. 3. Presumably uncorrelated broadband noise sources were excited in perforations in an aluminum plate with a thickness of 0.62 mm by a wall jet along the rear side of the plate. The perforations with a diameter of 2.38 mm were drilled into the plate in a V-shaped pattern. The acquisition time was 120 seconds with a sampling rate of 96 kHz. The data were measured with 24 microphones mounted on an octagonal plate with a size of about 56 cm. The distance between the source region and the microphone array was 30 cm. The angular range for the directivity of a point source in the plate with respect to all microphones is about $\pm$ 30 deg. The nine sources are likely very similar but the increasing distances between each pair between $\delta_4 = 8.8$ mm and $\delta_1 = 35.3$ mm enables an investigation of the spatial resolution of the localization methods. Results were shown for $1/12^{\text{th}}$ octave bands with center frequencies 4728 Hz, 7099 Hz, 8944 Hz and 15976 Hz. Figure 5 shows the results for 15976 Hz from their publication. These results will be used here for the comparison with SODIX.

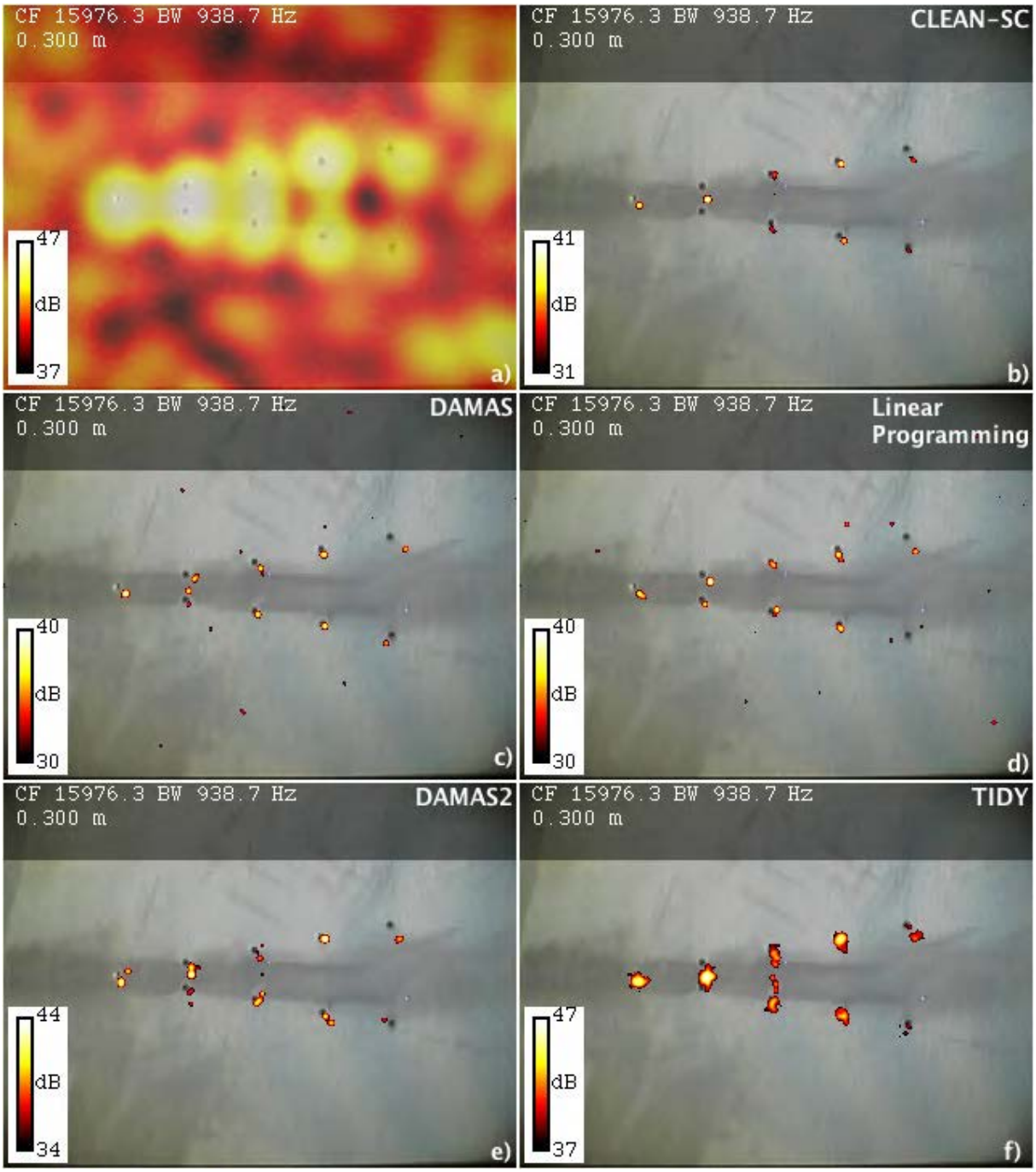

Figure 5: Beamforming and deconvolution results for a $1/12^{th}$ octave band around 16 kHz, taken from reference [9]

In order to minimize the influence of the finite plate of the array on the measured data, an amplitude and phase calibration was applied to the CSM. A calibrated loudspeaker was mounted for this purpose centrally in a distance of 2 m from the array and the ratio between the measured cross-spectral matrix and the theoretical one was determined and used to calibrate the measured

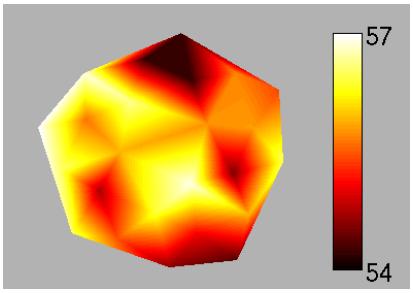

Figure 6: Measured SPL for 15516 Hz to 16406 Hz in dB as function of the microphone positions

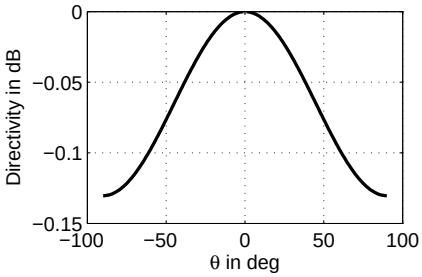

Figure 7: Directivity of a radiating piston (radius a=1.19 mm) in a rigid plate at 16 kHz

data. This calibration was taken into account in the preparation of all figures in this paper.

In the following evaluation of the SODIX results, the fit between the measured SPL and the SPL extrapolated from the SODIX source-model can be a useful measure for the quality of the source modeling with SODIX and of the data set. Figure 6 shows the measured SPL of the array microphones for the frequency band around 16 kHz. The measured SPL distribution shows local variations of about 3 dB. The levels are lowest on the top and the bottom edges of the array. This large variation is surprising, because in this set up, rather smooth changes in the sound field of a set of uncorrelated monopoles can be expected. The monopole assumption can be validated by approximating the existing sound sources as oscillating round pistons in a rigid wall. The sound pressure in the far-field of such a source has a directivity

$$L(\theta) = \frac{2J_1(ka\sin\theta)}{ka\sin\theta} \tag{14}$$

with J_1 the Bessel function of first kind, k the wave number, a the radius of the piston and θ the radiation angle relative to the piston axis. Figure 7 shows the logarithmic directivity for $f = 16\,\text{kHz}$ and $a = 1.19$ mm. The directivity shows negligible variations of less than 0.03 dB for $-30\,\text{deg} \leq \theta \leq 30\,\text{deg}$. Therefore, a directivity of the source can be excluded as explanation for the variations of the SPL of the array microphones and the variation in Fig. 6 must have more to do with the array and the calibration.

This is supported by results of Pott-Pollenske et al. [14] for the round ground-board microphone setup that is commonly used for flyover experiments. The interference pattern on this plate may change by ±5 dB when the angle of the incoming sound waves changes from 90 deg to 45 deg. The impedance jump between metal and the grass surface on the edge of the plate is the explanation.

One other possibility is that since the plate with the holes and the array were parallel, there could be some kind of standing waves between them. The plate was smaller in the vertical direction (See Fig. 3), so that a reverberation effect might be weaker at the top and bottom of the array that was not faced by the plate. Another shortcoming of the calibration, in addition to the fact that is was a finite-size speaker and was only in one point is the fact that the calibration was performed with the speaker at distance of 2 m (and was processed accordingly). Diffraction effects across the face of the array are likely different for a source at 0.3 m vs. 2 m.

3.2 SODIX parameters

The smoothing functions G_d and G_s were initially introduced into the SODIX method to change the ill-posed problem to a well-posed one and to improve the convergence to a physical solution. With experimental data from an aeroengine free-field-test it was shown, that the smoothing functions can suppress spurious sources, but naturally decrease the spatial resolution of the SODIX results [11]. With the current data set, the SODIX method was found to converge steadily without the use of the smoothing functions. This may be explainable by the fact that there are actually only 9 physical sources but 24 microphones. It was found here, as to be expected, that smoothing of the source distribution reduces the separation capability between sources. It can be concluded, that depending on the data set, the use of the smoothing function G_s may not always give a benefit. In this paper, the smoothing of the source distribution is always disabled by setting $\sigma_\mathrm{s} = 0$. The use of the directivity smoothing is investigated later in this section.

The input data for SODIX are 20 narrow-band frequencies (15516 Hz to 16406 Hz, 46.9 Hz frequency resolution) in the range of the $1/12^{\mathrm{th}}$ octave-band. The modeling of the source strengths in each frequency band is stopped after 200 iterations.

The source grid consists of $J = 9520$ directive point sources with a resolution of $1/8^{\mathrm{th}}$ of the Rayleigh limit ($\Delta x = \Delta y = 1.7\,\mathrm{mm} \approx 0.08\,\lambda$). The Rayleigh limit is about 30% larger than the Sparrow limit discussed in section 2. The number of directive source strengths that have to be determined is $J \cdot 24 = 228480$.

3.3 Results with no smoothing of the source directivities

Figure 8 shows SODIX results with no smoothing applied ($\sigma_\mathrm{d} = \sigma_\mathrm{s} = 0$). The overall modeled source distributions shown in subfigure 8a were calculated by summing up the directive source strengths over all microphones $\sum_M d_{jm}^4$. These results show that the sources are located at the correct positions but not all source pairs can be separated. A comparison with the results of the deconvolution methods shown in Fig. 5 demonstrates that these exhibit better spatial resolutions.

However, the sound-pressure levels at the microphone positions, that can be derived from the modeled source strengths, agree very well with the measured sound-pressure levels shown in Fig. 6. Subfigure 8b shows that the absolute difference is less than 0.5 dB for all microphones.

The important feature of the SODIX method is that it implies a directivity for each point source. The summation of directive source strengths d_{jm}^4 over sources j that are located in a particular source area (blue rectangles in Fig. 8a) gives the directivity of that source area. Subfigure 8c shows the directivities for all nine source areas with a 3 dB dynamic range. Note, that these plots do not show the extrapolated SPL at the microphone positions, but the directive source strengths normalized to 1 m distance from the sources as function of the microphone positions. The results show, that all directivities vary by more than 3 dB. In most cases, the particular maximum is directed towards the peripheral microphones. This agrees with the measured SPL distribution on the microphone array that was shown in Fig. 6. As discussed in section 3.1 this variation of the SPL values is unphysical but SODIX reconstructs the measured values if the smoothing G_d of the source directivities is switched off.

It can be noted that although the smoothing functions are disabled, the solution of the high number of unknowns converges and the modeled source distribution is reasonable.

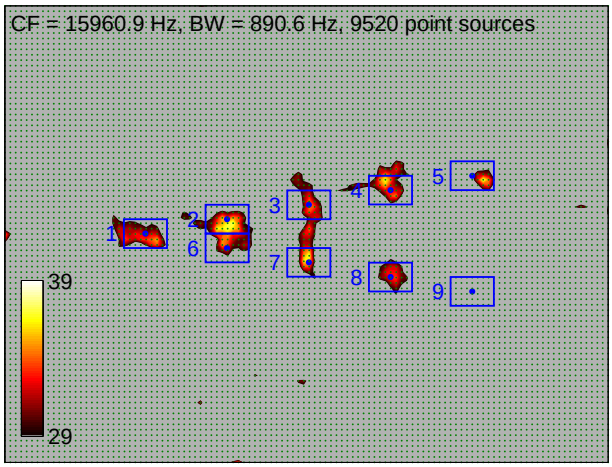

(a) *Source strengths $D^2_{jm} = d^4_{jm}$ summed up over all microphones M as function of source position in dB. Blue dots indicate real source positions, blue rectangles define source areas for directivity plots in subfigure (c)*

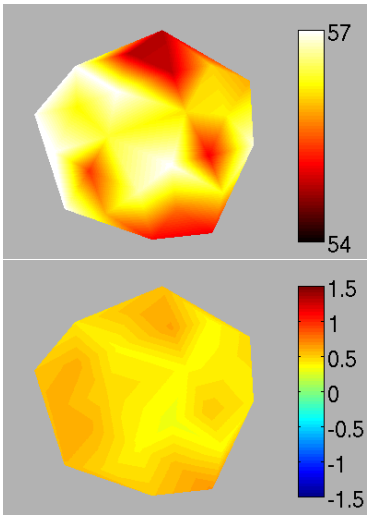

(b) *Modeled SPL at microphones in dB (top), deviation from measured SPL in dB (bottom)*

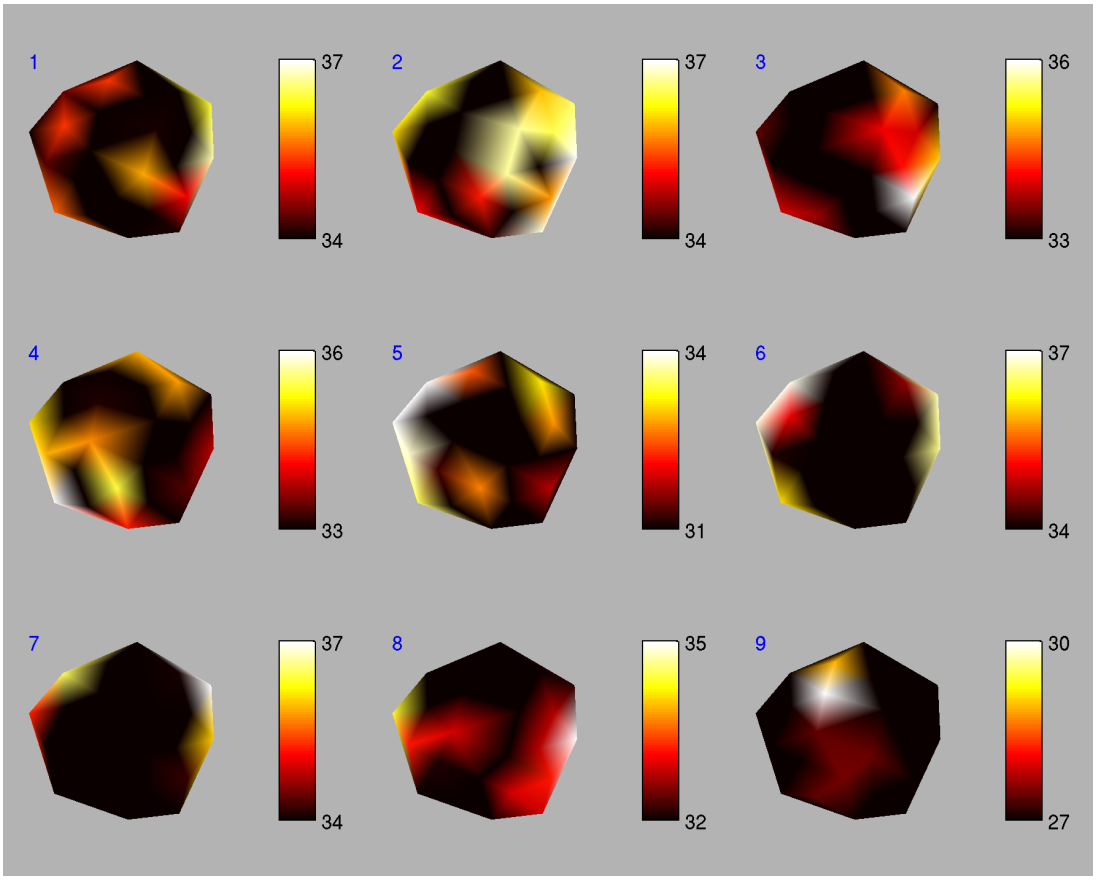

(c) *Source strengths $D^2_{jm} = d^4_{jm}$ summed up over the nine source areas (see subfigure (a)) in dB*

Figure 8: SODIX results for 15516 Hz to 16406 Hz, No smoothing ($\sigma_d = \sigma_s = 0$), the resolution of the source grid equals $1/8^{th}$ of the Rayleigh radius

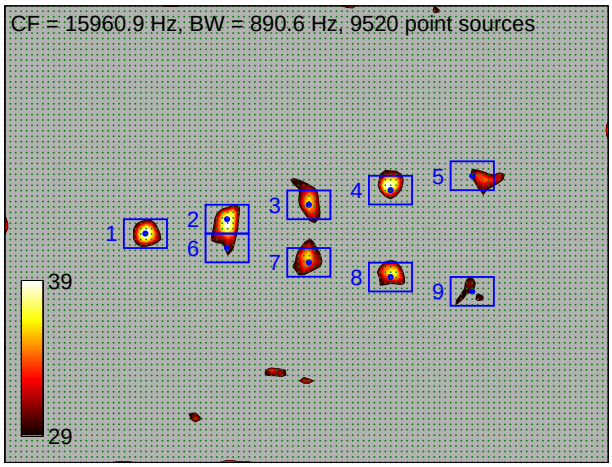

(a) Source strengths $D^2_{jm} = d^4_{jm}$ summed up over all microphones M as function of source position in dB. Blue dots indicate real source positions, blue rectangles define source areas for directivity plots in subfigure (c).

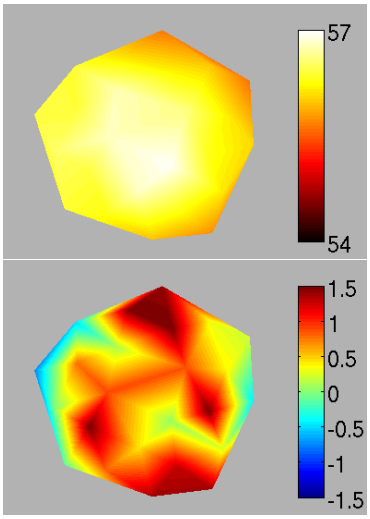

(b) Modeled SPL at microphones in dB (top), deviation from measured SPL in dB (bottom)

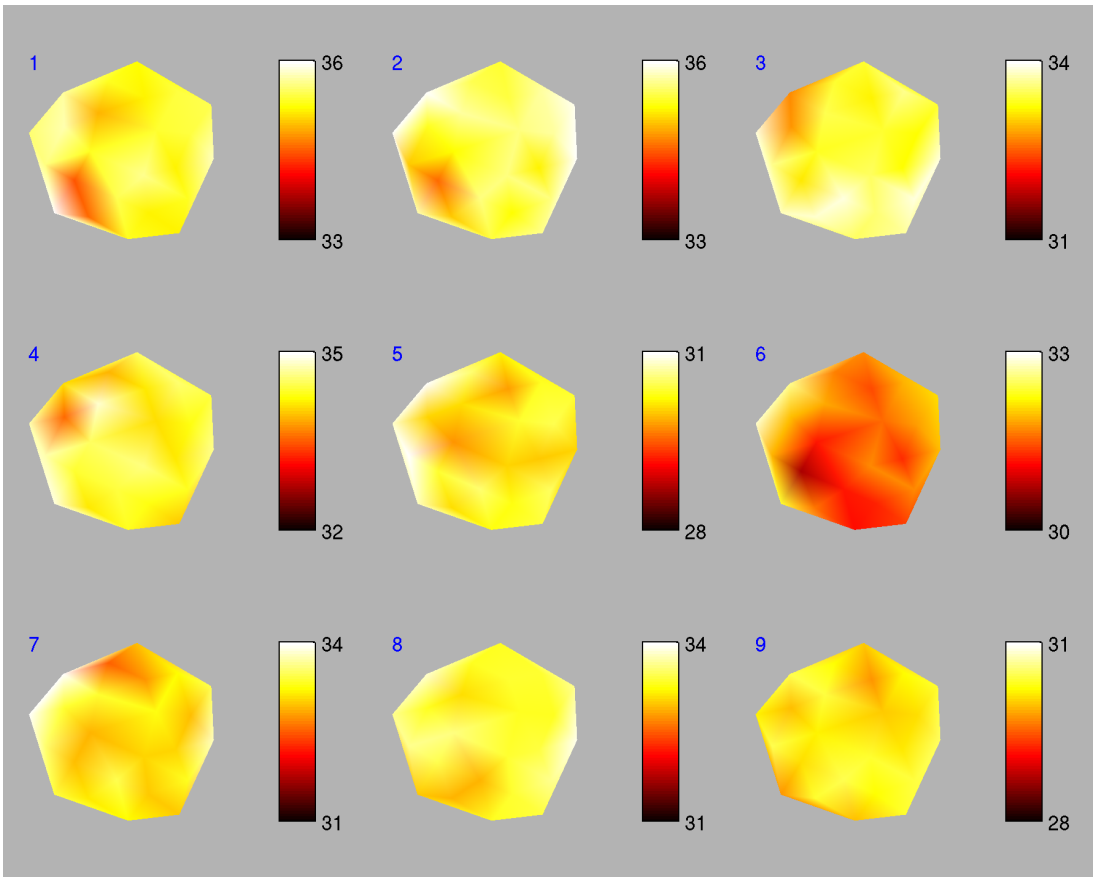

(c) Source strengths $D^2_{jm} = d^4_{jm}$ summed up in source areas (see subfigure (a)) in dB

Figure 9: SODIX results for 15516 Hz to 16406 Hz, Smoothing of the source directivities ($\sigma_d = 10^{-4}, \sigma_s = 0$), the resolution of the source grid equals $1/8^{th}$ of the Rayleigh radius

3.4 Results with smoothing of the source directivities

The influence of the smoothing of the source directivities is shown in Fig. 9. These results were computed with $\sigma_d = 10^{-4}$. Figure 9a shows that this smoothing did improve the resolution and that the results compare better with the results of the deconvolution methods shown in Fig. 5. The modeled directivities shown in Figs. 9b and 9c are much more uniform now in agreement with the physics discussed in section 3.1.

The difference between the measured and modeled SPL shown in the bottom part of Fig. 9b is caused by the unphysical variation of the measured data. It can be concluded that the smoothing has improved the result. A further increase of the smoothing parameter σ_d was tested but degraded the spatial resolution.

3.5 Computational costs

SODIX calculates individual source strengths from each of the J sources towards each of the M microphones. The number of unknowns N that have to be determined for each frequency band is therefore $N = JM$. This high number of unknowns results in long computation times. For the current data, the processing of one narrow-band (200 iterations) took about 3 hours on a 3.1 GHz eight core processor when no smoothing was applied. This time rose to 9 hours when the smoothing functions are used. The reason for this is the increased complexity of the cost function and the partial derivatives that have to be calculated during the minimization process.

Since the processing of each frequency band is independent of all other bands, the problem could easily be parallelized. The computation for all frequency bands would not take much longer than for a single frequency if one core could be reserved for each frequency band. A further improvement would be an adaptive source grid that starts with a low-density homogeneous source grid and increases the source density in areas with high source levels but also removes sources from the grid as they drop below a certain threshold.

4 CONCLUSIONS

The objective of this study was to compare the source localization program SODIX with advanced deconvolution methods. A data set was used that did not require the special capabilities of SODIX of being able to determine the directivities of the sources, since the comparison was performed for a frequency of 16 kHz, for which the directivities of the sources were uniform in the angular range covered by the microphone positions in the array. The results of SODIX shown in Fig. 9a are slightly inferior to the results of the deconvolution methods shown in Fig. 5.

SODIX revealed a problem with the data set. While the sound-pressure levels of all microphones were expected to be almost identical after amplitude and phase calibration with a loudspeaker they actually varied substantially by about 3 dB. Apparently, the amplitude and phase calibration did not completely consider the distortion by effects like scattering at the edges of the microphone array. The scattering at the edges of the source plate and the influence of reflections between the two plates were not taken care of at all. Smoothing of the directivities, which is a feature of SODIX, was sufficient to yield physically valid results. A small value for the smoothing parameter σ_d in the directivity smoothing function $\sigma_d G_d$ in Eq. (7) was used. Without smoothing SODIX tried to reproduce the actual sound pressure levels at the microphones with physically unrealistic source directivities and a nonphysically wider source distribution.

Directivity smoothing was introduced in SODIX to make the ill-posed problem to a well-posed one. However, it turned out that it was not required for a convergence of the solution for the given data set but necessary to achieve a physically realistic solution. Smoothing of the source distribution was also studied but no results are shown because a smooth source distribution was physically not valid. One might even conclude that the smoothing of the source distribution is not necessary and could be removed from the algorithm.

The current data-set was used for a first comparison of SODIX with advanced beamforming methods but it does not describe directive sources and this special capability of SODIX could not be tested. For a dedicated demonstration of the directivity modeling a new test set-up with directive sound sources would have to be designed in connection with a large array that spans a considerable angular range.

Because SODIX calculates an individual source strength from each source to each microphone the computational costs are high. The resolution of the SODIX source grid that was used here was only $1/8^{\text{th}}$ of the Rayleigh radius, while the results with advanced deconvolution methods shown in Fig. 5 were calculated with a much finer resolution of $1/24^{\text{th}}$ of the Rayleigh radius. It can be supposed that a finer SODIX source grid would produce results that come closer to the results with advanced deconvolution methods, but the computational costs would grow dramatically.

Improvements of the algorithm may be possible to reduce the computation times of SODIX. The solution could easily be parallelized over all existing cores of one machine or one cluster, since the processing of each frequency band is independent of all others. Alternatively, one could use the solution at frequency f_n as initial solution for frequency f_{n+1}. This would likely allow a lower number of iteration steps within the minimization process at frequency f_{n+1}. A further improvement would be an adaptive source grid that starts with a low-density homogeneous source grid and increases the source density in areas with high source levels but also removes sources from the grid as they drop below a certain threshold.

References

[1] D. Blacodon and G. Élias. "Level Estimation of Extended Acoustic Sources Using an Array of Microphones." In *9th AIAA/CEAS Aeroacoustics Conference, Hilton Head, South Carolina, May 12-14, 2003*. 2003. AIAA-2003-3199.

[2] D. Blacodon and G. Élias. "Level Estimation of Extended Acoustic Sources Using a Parametric Method." *Journal of Aircraft*, 41, 1360–1369, 2004. doi:10.2514/1.3053.

[3] T. F. Brooks and W. M. Humphreys, Jr. "A Deconvolution Approach for the Mapping of Acoustic Sources (DAMAS) Determined from Phased Microphone Arrays." In *10th AIAA/CEAS Aeroacoustics Conference, Manchester, Great Britain, May 10-12, 2004*. 2004. AIAA-2004-2954.

[4] T. F. Brooks and W. M. Humphreys, Jr. "A deconvolution approach for the mapping of acoustic sources (DAMAS) determined from phased microphone array." *J. Sound Vib.*, 294(4-5), 856–879, 2006. doi:10.1016/j.jsv.2005.12.046.

[5] S. Brühl. "Source density modelization of 2D array measurement data." Technical Report 1F 7M11 T1.DB (DeuFraKo, Annex K2), DeuFraKo, 1997.

[6] S. Brühl and A. Röder. "Acoustic noise source modelling based on microphone array measurements." *J. Sound Vib.*, 231(3), 611–617, 2000. doi:10.1006/jsvi.1999.2548.

[7] R. P. Dougherty. "Extensions of DAMAS and Benefits and Limitations of Deconvolution in Beamforming." In *11th AIAA/CEAS Aeroacoustics Conference, Monterey, California, May 23-25, 2005*. 2005. AIAA-2005-2961.

[8] R. P. Dougherty and G. Podboy. "Improved Phased Array Imaging of a Model Jet." In *15th AIAA/CEAS Aeroacoustics Conference (30th AIAA Aeroacoustics Conference), 11 - 13 May 2009, Miami, FL*. 2009. AIAA-2009-3186.

[9] R. P. Dougherty, R. C. Ramachandran, and G. Raman. "Deconvolution of sources in aeroacoustic images from phased microphone arrays using linear programming." In *19th AIAA/CEAS Aeroacoustics Conference, Berlin, Germany, 27th-29th May 2013*. 2013. AIAA-2013-2210. doi:10.2514/6.2013-2210.

[10] K. Ehrenfried and L. Koop. "Comparison of Iterative Deconvolution Algorithms for the Mapping of Acoustic Sources." *AIAA Journal*, 45(7), 1584–1595, 2007. doi:10.2514/1.26320.

[11] S. Funke, A. Skorpel, and U. Michel. "An extended formulation of the SODIX method with application to aeroengine broadband noise." In *18th AIAA/CEAS Aeroacoustics Conference (33rd AIAA Aeroacoustics Conference), June 4 -6, 2012, Colorado Springs, Colorado, USA*. 2012. doi:10.2514/6.2012-2276.

[12] U. Michel and S. Funke. "Inverse method for the acoustic source analysis of an aeroengine." In *Proceedings on CD of the 2nd Berlin Beamforming Conference, 19-20 February, 2008*. GFaI, Gesellschaft zu Förderung angewandter Informatik e.V., Berlin, 2008. ISBN 978-3-00-023849-9. BeBeC-2008-12. URL `http://bebec.eu/Downloads/BeBeC2008/Papers/BeBeC-2008-12_Michel_Funke.pdf`.

[13] U. Michel and S. Funke. "Noise Source Analysis of an Aeroengine with a New Inverse Method SODIX." In *14th AIAA/CEAS Aeroacoustics Conference, Vancouver, BC, Canada, May 5-7, 2008*. 2008. AIAA-2008-2860.

[14] M. Pott-Pollenske, W. Dobrzynski, H. Buchholz, S. Guérin, and U. Finke. "Airframe noise characteristics from flyover measurements and predictions." In *12th AIAA/CEAS Aeroacoustics Conference (27th AIAA Aeroacoustics Conference), Cambridge, Massachusetts, May 8-10, 2006*, pages AIAA–2006–2458. 2006.

[15] C. E. Rasmussen. *Evaluation of Gaussian Processes and other Methods for Non-Linear Regression*. Ph.D. thesis, Graduate Department of Computer Science in the University of Toronto, 1996.

[16] E. Sarradj. "A fast signal subspace approach for the determination of absolute levels from phased microphone array measurements." *J. Sound Vib.*, 329(9), 1553–1569, 2010. doi:10.1016/j.jsv.2009.11.009.

[17] P. Sijtsma. "CLEAN Based on Spatial Source Coherence." In *13th AIAA/CEAS Aeroacoustics Conference, Rome, Italy, May 21-23, 2007*, pages AIAA–2007–3436. 2007. AIAA Paper 2007-3436.

[18] P. Sijtsma. "CLEAN based on spatial source coherence." *International Journal of Aeroacoustics*, 6, 357–374, 2007.

[19] P. Sijtsma. "Tutorial: Improving resolution with CLEAN-SC." In *Proceedings on CD of the 2nd Berlin Beamforming Conference, 19-20 February, 2008*. 2008. ISBN 978-3-00-023849-9. URL `http://bebec.eu/Downloads/BeBeC2008/Presentations/BeBeC-2008_Sijtsma_CLEAN_SC.pdf`.